Prepared for submission to JINST

International Conference on Fusion Reactor Diagnostics
6-10 September, 2021
Villa Monastero, Varenna, Italy

An ultrahigh-bandwidth Phase Contrast Imaging system for fusion plasmas

A. Marinoni, J.C. Rost, M. Porkolab and R. Seraydarian

Massachusetts Institute of Technology, Plasma Science and Fusion Center
Cambridge, MA 02139, USA

E-mail: marinoni@mit.edu

Abstract: A novel Phase Contrast Imaging system that uses probing light in the near infrared region has been developed to image electron density fluctuations in fusion plasmas. As compared to standard systems operating in the mid infra-red region, the spectral response of the system is extended in wave-number and frequency response by 7 and 100 times, respectively. The internal structure of turbulence and radio-frequency waves is therefore accessible across an unprecedented wavelength and frequency range, extending into the electron gyro-radius scale and the GHz frequency region.

Keywords: Plasma diagnostics - interferometry, spectroscopy and imaging; Nuclear instruments and methods for hot plasma diagnostics

Contents

1 Introduction 1

2 Implementation and results 3

3 Conclusions 6

1 Introduction

The Phase Contrast Imaging (PCI) method is an optical technique that converts phase shifts induced on the wavefront of probing light travelling through a transparent medium into amplitude variations at the image plane. Invented in the 1930s by F. Zernike [1], who proved its superior sensitivity compared to competing methods used in cellular microscopy, its application to plasmas was pioneered by M. Presby and D. Finkelstein in the late 1960s [2]. In the late 1980s, successful experiments on magnetically confined fusion grade plasmas from H. Weisen [3] prompted its worldwide installation on tokamaks [4–9] as well as stellarators [10–12]. In very simplistic terms, the PCI technique can be described as an internal reference interferometer, i.e. for which both the test and the reference legs travel through the object, that measures the spatial distribution of refraction index by imaging the probing light beam onto an array of detectors. In the specific case of probing light frequency much higher than any plasma frequency and for spatial inhomogeneities larger than the probing light wavelength, diffraction occurs in the Raman-Nath regime [13] and the plasma behaves as a transparent object which induces phase shifts that can be expressed as

$$\phi(\mathbf{x},t) = \lambda_0 r_e \int_a^b dx_{\parallel}\, n_e(\mathbf{x},t), \tag{1.1}$$

where λ_0 is the wavelength of the probing light in vacuum, r_e is the classical electron radius, n_e is the plasma electron density and the parallel spatial coordinate refers to the propagation direction of the probing laser beam. The total phase shift, ϕ, is usually decomposed into a component given by the stationary plasma density, $\phi_0(\mathbf{x})$, and that due to fluctuations, $\tilde{\phi}(\mathbf{x},t)$, which is usually much smaller than the former. As a consequence, the probing light electric field E_0 becomes equal to

$$E_{tot}(\mathbf{x},t) = E_0 e^{\imath\phi(\mathbf{x},t)} = E_0 e^{\imath\phi_0(\mathbf{x})} e^{\imath\tilde{\phi}(\mathbf{x},t)} \simeq E_{\phi_0}[1 + \imath\tilde{\phi}(\mathbf{x},t)]. \tag{1.2}$$

Equation 1.2 states that the total electric field, E_{tot}, is composed of two components that are $\pi/2$ phase shifted with respect to each other: the field of the reference beam, E_{ϕ_0}, and that of the test beam that has interacted with the fluctuating plasma density, $E_{\phi_0}\imath\tilde{\phi}$. The PCI method employs the fact that the two legs propagate at finite angles with respect to each other and separates them in a suitable focal plane of the imaging system. An additional $\pi/2$ phase shift is then applied by having the reference beam impinge onto an appropriately size groove dug in an otherwise flat optical

component, called *phase plate*, that can be either reflective of transmissive. Additionally, in order to increase the contrast between the two components, the intensity of the reference beam is usually attenuated by a factor $\rho < 1$ in the groove. The *invisible* phase shifts are thereby made *detectable* as variations in brightness and, to first order in the perturbed phase, can be expressed by relation

$$|E(\mathbf{x}_\perp, t)|^2 \simeq |E_{\phi_0}|^2 \left[\rho \pm 2\tilde{\phi}(\mathbf{x}_\perp, t)\right] . \tag{1.3}$$

Equation 1.3 shows that the sensitivity of a PCI system is a factor $2/\rho$ higher than that of a comparable homodyne interferometer operated in optimal detection mode, i.e. with the two legs exactly out of phase, with other parameters being equal.

Motivation for a near infra-red (NIR) PCI system Worldwide PCI diagnostics installed on magnetic fusion devices work in the mid infra-red (MIR) spectral region by employing probing CO_2 lasers that oscillate on the 10.59 µm wavelength. This choice was a compromise between various considerations. A shorter probing wavelength more easily satisfies the approximations required by the PCI method, e.g. low angle scattering and the Raman-Nath regime, and it reduces refraction effects. On the other hand, optical aberrations and the quality (as well as cleanliness) of optical components have less of a detrimental effect on the image at longer wavelengths. Additionally, the focal spot of a given focusing optic increases at increasing wavelength, which eases manufacturing tolerances on the width of the groove and reduces the power density of the reference beam therein. The probing wavelength sets the highest limit for both the wave-number and frequency response of the system. Indeed, the angle that separates the directions of propagation of the test and reference beams is linearly proportional to the wave-number of the scattering radiation; this, for any given probing wavelength and size of the probing beam, sets an upper limit to the wave-vectors that are not clipped by any of the optics. On fusion grade machines this limit is usually around $k = 20\,\mathrm{cm}^{-1}$ which, for typical values of the ion larmor radius, corresponds to the region where ITG&TEM instabilities are active. The frequency bandwidth is given by the rise time of the detectors. In the case of light at 10.6 µm wavelength, arrays of HgCdTe detectors are employed to image the spatial structure of the perturbed electron density. In order to achieve high sensitivity to small signal from turbulence, the detectors are cryogenically cooled at the temperature of liquid nitrogen to minimize noise due to thermally excited current carriers. As a result, the 3dB point is usually located at frequencies less than one or a few MHz, depending on whether the detectors are operated in the photoconductive or photovoltaic regime. The study of faster phenomena therefore requires the use of optical heterodyning techniques which employ suitable modulators to sinusoidally vary the intensity of the probing laser beam at a frequency close to that of the wave to be detected, so that the resulting beating frequency falls within the bandwidth of the detector. Although this technique proved to be robust on the Alcator C-mod tokamak [14, 15], it requires dedicated hardware components, careful alignment through the modulator as well as prior knowledge of the frequency of the wave to be measured.

In this work we developed a PCI system at 1.55 µm, wavelength at which detectors have their peak sensitivity, to deliver three key advantages. First, the angle between the test and reference beams decreases by a factor of seven which, for a given maximum value permitted by the aperture stop, gives access to higher wave-numbers well into the ETG instability range. Alternatively, any given fluctuation wave-number can be collected by smaller optics or by the same size optics located 7

times further away from the vacuum vessel. The latter property is of interest in large scale devices where long beam paths from the diagnostic to the vessel hall will be required; for example, while total laser beam paths of 15 m to 30 m are typical in current devices, optical diagnostics in ITER are located in a different building leading to beam paths of the order of 100 m[1]. Second, considerable progress by R&D programs in the telecommunication and military sectors made low noise room temperature detector arrays readily available with GHz frequency bandwidth, i.e. two to three orders of magnitude wider than that of existing systems in the MIR region, which allows one to directly digitize data without using complex heterodyning detection schemes. Although the signal amplitude linearly decreases with shorter probing light wavelength, as can be seen in Eq. 1.1, the SNR does not degrade thanks to the fact that, when compared to cryogenically cooled HgCdTe detectors, InGaAs detectors feature a two order of magnitude higher normalized detectivity D^* and a larger saturation power, which significantly lower detector and shot noise. Third, the rising NIR market contributed to drive down prices and furbish inventory. As a result, high quality lasers, optical components and imaging tools suitable for remote alignment tasks are available off-the-shelf and at a much lower price. Maintenance overhead is also reduced as detectors are not cryogenically cooled.

2 Implementation and results

In order to characterize the system response at shorter probing wavelength, a prototype was designed and installed on an optics table to allow flexible testing of components and associated effects on the quality of the laser. The nature of the project implied cost effective solutions while obtaining adequate response. In the following we describe the main components that were used or had to be manufactured for the system to properly work.

Phase plates In order to provide the desired $\pi/2$ phase shift between the reference and test beams, the depth of the groove in reflecting phase plates must be approximately equal to one-eighth of the probing light wavelength, one fourth for a transmitting plate, which entails stricter tolerances when using a shorter wavelength. Accuracy on the groove's width is far less critical as the size of the beam focal spot can be adjusted to match the width of the groove by using an appropriate optical layout. Suitable phase plates were successfully developed for light at 1.55 µm with two methods for a cost of a few thousands of US dollars: masked coating and a micro-technology lift-off process. The first method produced several phase plates made of N-BK7, ZnSe, Ge and Al substrates with grooves 254 and 762 µm wide. Blanks were installed in an appropriate recess and covered by a wire which, after aluminum coating was deposited in a standard evaporator, was removed to expose the groove. In order to achieve a uniform groove with nearly right angle cliffs, flat ribbons were preferred to round wires and were spring loaded to provide tight contact with the surface to be coated. In view of the tension provided by the springs, the ribbons are made of 304VM stainless steel which has a more favorable stress-strain curve than aluminum. An appropriate jig was built to accommodate all substrates in a single coating run. While this procedure minimized the fixed cost associated with

[1]Readers unfamiliar with typical layouts of the PCI diagnostic in current experiments are referred to Figure 3-1 in [16], where that on the DIII-D tokamak is displayed. A description of the 10.6 µm interferometer prototyped for ITER and installed on DIII-D is displayed in [17] Figure 2.

the use of the evaporator, it also resulted in some variability in the depth of the grooves, which were measured to be within 10-20% of the desired value. The second method was carried out by the Materials Research Institute of Penn State University, PA, USA. The procedure consisted of two phases: a photomask was created for patterning the groove, followed by the development of a lift-off process for fabricating the final device. The resulting groove depth was measured to be within 2% of the desired value, using both interferometric techniques and optical measurements made with the Keyence VK-X1000 confocal microscope. The latter also revealed a much steeper slope of the edges of the grooves manufactured with the lift-off technique. Indeed, while masked-coated grooves fall-off from peak to valley in about 60 µm, the lift-off method achieves that in approximately 2 µm, which improves the system response near the low wave-number cut-off.

Other components and layout The laser source consists of a fiber-coupled laser diode whose output power, for flexibility in testing, can be continuously varied up to 100 mW (Emcore model 1782 DWDM), which was the minimum power deemed necessary. In order to obtain high-quality beam in a single longitudinal mode with a narrow spectral bandwidth, laser diodes delivering more than 20 mW require a temperature controller, rather than a heat sink, and a low-noise current driver. This was accomplished by procuring an appropriate controller (Arroyo Instruments 685-01 ComboPak). The laser beam exiting from the fiber is highly divergent and, when collimated using regular lenses, showed large diffraction patterns. A fiber-optic collimator (Thorlabs F810APC-1550) yielded a gaussian beam with quality factor $M^2 = 1.6$ and eccentricity equal to 0.34. The beam quality could be somewhat improved by spatially filtering the beam with a pinhole in a focal plane, but this was found to provide negligible effect to the measured signal. After the fiber collimator, standard 2-inch, AR/AR coated, N-BK7 lenses are used to expand the beam to the desired width, focus it on the phase groove and create the image plane. A 16-element InGaAs detector array (Hamamatsu G12430-016D) was procured to reconstruct the wavenumber of sound waves used to probe the system response. The detector noise is given by a specific detectivity $D^* = 5 \cdot 10^{12}$ cm $Hz^{1/2}$ W^{-1} while the 3 dB point is located at 30 MHz.
Before being digitized on a four channels oscilloscope, the signal is amplified by two-stage transimpedance amplifiers mounted on a perforated busboard. The amplifiers are DC coupled to allow easy centering of the beam on the detector. In a production system the SNR would be increased by mounting amplifiers and the detector on a printed circuit board; additionally, the amplifiers would be AC coupled to optimize the use of the dynamic range. As the PCI method is capable of measuring density waves in air as well as plasma, the response of the system was tested by having ultrasound waves of known frequency propagate across the expanded and collimated laser beam. The size of the expanded beam is such that the low wavenumber cutoff of the system is $k_{min} = 3$ cm^{-1}.

System response When using ultrasound waves generated by a transducer at fixed frequency, all detector channels show comparable signal amplitudes and constant phase shifts, thus demonstrating basic PCI functionality. The amplitude of the signal is measured to be 30% less than the expected value based on the responsivity of the detector, the transimpedance gain of the amplifiers and the expected perturbed index of refraction of the air. It was not possible to measure the intensity of the ultrasound waves with a calibrated microphone; rather, it was inferred from previous measurements [16]. Uncertainties in the positioning of the transducer with respect to the laser and a

plausible degradation of the transducer response over a ten year period are likely to explain the 30% discrepancy.

Measurements in a continuous frequency range between 20 and 250 kHz are carried out using an ultrasonic speaker. Figure 1a displays the reconstructed wave-number vs that of the perturbing sound wave, estimated from the measured channel-to-channel phase shift. The linear behavior across the entire frequency range verifies that the perturbation is correctly reproduced on the detector, showing no distortion. Since each frequency tests a different portion of the phase plate, this linear behavior demonstrates that the flatness and uniformity of the phase plate coating are adequate. The intensity of the perturbation produced by the speaker decreases strongly with decreasing wavelength, which explains the larger noise at high frequency.

Since the PCI cannot properly image wavelengths larger than the laser beam diameter, its response function decreases monotonically to zero as the wavelength of the probing ultra sound increases [3]. This behavior is reproduced by the measurements in fair agreement with the expected response, as displayed in figure 1b.

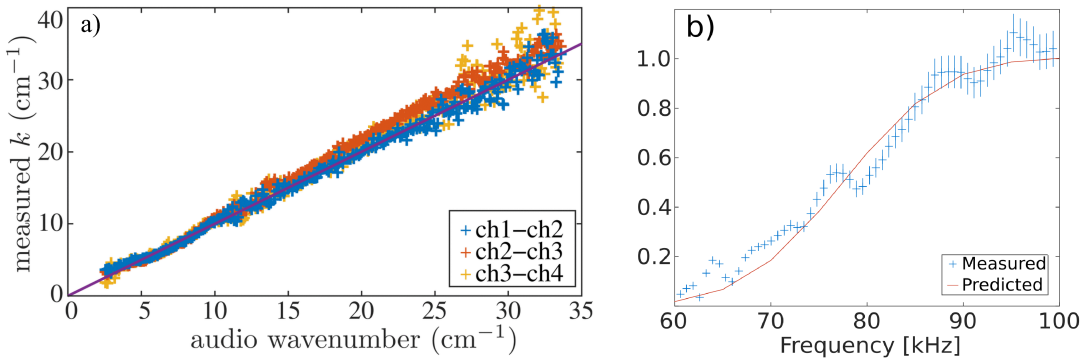

Figure 1. a) Reconstructed vs probing wave-numbers of the ultra sound wave. b) Measured and expected normalized PCI response function vs the frequency of the probing ultra sound wave.

Noise The system noise was quantified using specifications listed by the manufacturer of every component used. Thermal noise in the resistors of the preamplifier and current noise in the OP-27 used accounted for 59 nV Hz$^{-1/2}$. Disturbances from ambient fields and limitations in the construction of the busboards are expected to increase this figure and should be reduced in production systems with properly shielded printed circuit boards. Detector noise accounted for 0.09 nV Hz$^{-1/2}$. Shot noise due to the quantum nature of light contributed, at the power level used, 83 nV Hz$^{-1/2}$ while laser amplitude fluctuation noise (RIN) is specified to be no larger than 155 dB Hz^{-1}, corresponding to 51 nV Hz$^{-1/2}$. Quantization noise is significant due to the low bit depth of the oscilloscope, as compared to standard digitizers commonly used in experiments, and amounts to 50 nV Hz$^{-1/2}$. Noise at frequencies higher than 10 kHz was found to be roughly independent of laser power and within a factor of two of the minimum expected noise, while that at lower frequency was found to increase with increasing laser power and exceeded the expected level by a factor of 20. These tests indicate that a production system would benefit from a scientific grade, low noise laser. Additionally, the high noise at low frequency might be also due to the fact that testing had to be carried out in a workspace with significant levels of vibrations caused by heavy

machinery. In this respect, a vibration insulated optics table and an active system to compensate for vibrations are expected to decrease the low frequency noise.
While all measurements described above were carried out using scientific grade mirrors with surface flatness specified at $\lambda/10$ @ 633 nm, the impact of surface imperfections was estimated by replacing one at a time the high quality mirrors with lower grade $\lambda/4$ mirrors. While the signal amplitude slightly decreases with lower quality mirrors, the channel-to-channel phase difference is unaffected. This indicates that optical imperfections do not distort the signal, to the degree tested.

3 Conclusions

The Phase Contrast Imaging method used to detect electron density fluctuations in plasmas has been extended from the Mid- to the Near-InfraRed spectral region. The reduced probing wavelength allows one to either extend the measured signal to higher wave-numbers into electron gyro-radius scales, and/or use smaller collection optics. The frequency bandwidth is increased by two orders of magnitude, up to GHz frequency range, thereby enabling direct digitization of radio-frequency waves. Custom phase plates have been developed using two different methods, both of the provided correct functioning of the system. The overall noise figure is close to expected values based on the components used. In addition to the wider wave-number&frequency response, lower maintenance overhead and easier accessibility to alignment tools makes this system suitable for operation in future large scale devices where access to the machine hall will be restricted.

Acknowledgments

Work supported under US-DoE award DE-SC0018095. The authors acknowledge Dr. E.M. Davis for valuable assistance, A. Bordeon from Keyence for the microscopic measurements, as well as MicroTek Corp (NJ) and Metallurgical Solutions (CA) for providing the high quality ribbons.

References

[1] F. von Zernike, *Beugungstheorie des schneidenver-fahrens und seiner verbesserten form, der phasenkontrastmethode*, *Physica* **1** (1934) 689.

[2] H.M. Presby and D. Finkelstein, *Plasma phasography*, *Review of Scientific Instruments* **38** (1967) 1563 [https://doi.org/10.1063/1.1720602].

[3] H. Weisen, *The phase contrast method as an imaging diagnostic for plasma density fluctuations (invited)*, *Review of Scientific Instruments* **59** (1988) 1544 [https://doi.org/10.1063/1.1140193].

[4] S. Coda, M. Porkolab and T.N. Carlstrom, *A phase contrast interferometer on DIII-D*, *Review of Scientific Instruments* **63** (1992) 4974 [https://doi.org/10.1063/1.1143516].

[5] E. Lo, R. Nazikian, D. Stutman, W. Choe and R. Kaita, *Calibration and test of the tangential phase contrast imaging diagnostic on CDX-U*, *Review of Scientific Instruments* **68** (1997) 1206 [https://doi.org/10.1063/1.1147883].

[6] R. Chatterjee and G.A. Hallock, *First results from the phase contrast imaging system on text-u*, *Review of Scientific Instruments* **68** (1997) 676 [https://doi.org/10.1063/1.1147717].

[7] A. Mazurenko, *Phase Contrast Imaging on the Alcator C-Mod tokamak*, Ph.D. thesis, Dept. of Physics, Massachusetts Institute of Technology, Cambridge, MA, USA, 2001.

[8] A. Marinoni, S. Coda, R. Chavan and G. Pochon, *Design of a tangential phase contrast imaging diagnostic for the TCV tokamak*, *Review of Scientific Instruments* **77** (2006) 10E929 [https://doi.org/10.1063/1.2222333].

[9] Y. Yu, S. Gong, M. Xu, C. Xiao, W. Jiang, W. Zhong et al., *Calibration of phase contrast imaging on HL-2A tokamak*, *Journal of Instrumentation* **12** (2017) C10005.

[10] K. Tanaka, K. Matsuo, K. Goto, M. Bowden, K. Muraoka, T. Furukawa et al., *Applicability of laser phase contrast method for the measurements of electron density fluctuations in high-temperature plasmas*, *Jpn. J. Appl. Phys.* **31** (1992) 2260.

[11] K. Tanaka, L.N. Vyacheslavov, T. Akiyama, A. Sanin, K. Kawahata, T. Tokuzawa et al., *Phase contrast imaging interferometer for edge density fluctuation measurements on LHD*, *Review of Scientific Instruments* **74** (2003) 1633 [https://doi.org/10.1063/1.1538361].

[12] Z. Huang, E. Edlund, M. Porkolab, J.-P. Bähner, L.-G. Böttger, C. v. Sehren et al., *The Wendelstein 7-X phase contrast imaging diagnostic*, *JINST* **16** (2021) P01014.

[13] C.V. Raman and N.S. Nagendra Nath, *The diffraction of light by high frequency sound waves: Part I*, *Proc. Indian Acad. Sci.* **A2** (1935) 406.

[14] E. Nelson-Melby, M. Porkolab, P.T. Bonoli, Y. Lin, A. Mazurenko and S.J. Wukitch, *Experimental observations of mode-converted ion cyclotron waves in a tokamak plasma by phase contrast imaging*, *Phys. Rev. Lett.* **90** (2003) 155004.

[15] N. Tsujii, M. Porkolab, P.T. Bonoli, E.M. Edlund, P.C. Ennever, Y. Lin et al., *Validation of full-wave simulations for mode conversion of waves in the ion cyclotron range of frequencies with phase contrast imaging in Alcator C-Mod*, *Physics of Plasmas* **22** (2015) 082502 [https://doi.org/10.1063/1.4927912].

[16] J.R. Dorris, *Phase Contrast Imaging Measurements and Modeling of Short Wavelength Turbulence in the DIII–D Tokamak*, Ph.D. thesis, Dept. of Physics, Massachusetts Institute of Technology, 2010. Available at https://dspace.mit.edu/handle/1721.1/62872.

[17] M.A. Van Zeeland, T.N. Carlstrom, D.K. Finkenthal, T. Akiyama, R.L. Boivin, A. Colio et al., *Tests of a full-scale ITER toroidal interferometer and polarimeter (TIP) prototype on the DIII-D tokamak (invited)*, *Review of Scientific Instruments* **89** (2018) 10B102 [https://doi.org/10.1063/1.5037461].